Thermal stability, glass-forming ability, and fragility nature of phase-change alloys of $Se_{90}Pb_{10-x}Sn_x$ ($0 \le x \le 8$) system

Mousa M. A. Imran[1] · Omar A. Lafi[1] · Amal Rabah[1] · A. Al-Bqoor[1] · A. Dahshan[2] · H. I. Elsaeedy[2] · N. Mehta[3]

Abstract

Bulk $Se_{90}Pb_{10-x}Sn_x$ ($x = 0, 2, 4, 6$, and 8) glassy alloys have been obtained by quenching technique, where x indicates the atomic mass percentage (at. mass%) of tin. The differential scanning calorimeter (DSC) technique is used under non-isothermal conditions to determine different characteristic temperatures such as the glass transition temperature T_g, on-set and peak crystallization temperatures T_c and T_p, and melting temperature T_m. The thermal stability parameter of current ternary $Se_{90}Pb_{10-x}Sn_x$ glasses exhibits A nonlinear compositional dependence with a maximum value for x = 8 at. mass% of Sn. The mean values of the crystallization rate ($<K_p>$) are lowest at $x = 2$ and 8, suggesting that a long time is required for these two compositions to fully crystallize. As a result, their stability against devitrification is at its highest, whereas the composition containing 6 at. mass% of Sn has the highest rate of crystallization and the lowest stability against devitrification.

Keywords Glass transition · Crystallization · Activation energy · Rate constant

Introduction

Glass is an inorganic material that is often created from a liquid state by rapidly cooling it down to a solidified state with a steady rise in viscosity. This prevents crystallization from occurring [1]. The prevention of crystallization implies that the resulting glassy rigid material is amorphous and characterized by short-range order. Oxide glasses, which are used in our daily lives, are insulators with band gap energy of more than 6 eV. Chalcogenide glasses, on the other hand, are unique varieties of glasses having chalcogens from group VI (B) and other elements from other groups of the periodic table. Further, their energy band gap exists in the range of 1–3 eV and therefore chalcogenide glasses are semiconductors [2]. In these glasses, the physical characteristics of the resultant semiconductor alter continuously as a result of the vast composition range of glass production. These materials, whose properties are customizable, serve as the foundation for the development of manufacturing technology in the field of solid-state devices. This approach opens new avenues for technological application beyond their current range of practical uses [3–5].

When growth and nucleation processes take place, the glassy alloy's resistance to devitrification is measured by its thermal stability (TS) [6]. The tendency of glass-forming is the term (GFA) indicating the ease with which a melt can be cooled without generating crystals during the preparation process [7]. An explanation of GFA and the characteristics of the glassy phase in glassy materials is one of the main issues in condensed matter physics that has not yet been fully resolved. GFA and TS are independent and related to two properties of any glass. These two parameters have been widely studied in the literature for chalcogenide glasses [8–11]. The studies [8–11] show that TS and GFA are related to each other and the composition of the glass. Consequently, valuable information can be collected to determine their utility in suitable practical applications.

On the other hand, according to Angell's theory, the definition of fragility is the rate at which a supercooled liquid's viscosity increases at the glass transition temperature while cooling [12]. Angell has classified glass-forming liquids into two classes: strong liquids and fragile liquids, depending on their fragility. According to the

✉ N. Mehta
dr_neeraj_mehta@yahoo.co.in

1 Physics Department, Faculty of Science, Al-Balqa Applied University, Al-Salt 19117, Jordan

2 Department of Physics, College of Science, King Khalid University, 61413 Abha, Saudi Arabia

3 Physics Department, Institute of Science, Banaras Hindu University, Varanasi 221005, India

aforementioned classification, the durability of the intermediate range order in the liquid increases when the temperature starts rising above its glass transition to reach the temperature at which it melts [13]. Strong glass-forming fluid viscosity exhibits Arrhenius temperature dependency with an insignificantly varying prominent activation energy. The perceived activation energy for the viscous stream, in contrast, increases sharply from an extremely small value beyond the melting temperature toward an extremely large value as the glass transition approaches the viscosity of delicate liquids that form fragile glasses [14].

Several quantitative approaches have been used to evaluate the level of TS, GFA, and fragility nature of the glassy alloys. Most of these methods are founded on typical temperatures for instance the melting temperature (T_m), glass transition temperature (T_g), and on-set and peak crystallization temperatures (T_c and T_p). The approach that is typically used to determine the aforementioned temperatures involves scanning the samples under non-isothermal circumstances by using a differential scanning calorimeter (DSC) at different heating rates. In the present work, several parameters of TS, GFA, and fragility nature in $Se_{90}Pb_{10-x}Sn_x$ ($0 \leq x \leq 8$) samples have been evaluated. We have chosen the Se–Pb–Sn system since researchers have reported their usefulness in thermo-electric and thermo-photovoltaic applications [15, 16]. Zobac et al. also reported that the Pb–Se–Sn ternary system plays a significant role in the development of materials for thermoelectric applications [17]. Studies indicate that an optimal range of lead content x in selenium to maintain the glassy character of the $Se_{100-x}Pb_x$ system is 0.1–10. The excessive lead content (i.e., composition higher than 10 at. mass%) in selenium may lead to strong possibilities the phase separation and crystallization [18]. The addition of light element tin at the cost of heavy element lead makes the formation of the glass convenient at manual cooling rates during the quenching of the melt [17]. This is the reason behind the chosen compositions of Pb and Sn in the present ternary system.

The Dietzel temperature differential ($T_c - T_g$), the stability parameters (H_g and S), the glass transition activation energy E_t, and the mean rate factor (K_p) of crystallization have all been calculated to study the transition state. The lowered glass transition temperature T_{rg} and the Hruby parameter H_R have also been calculated to further study GFT. The fragility index F_i has also been obtained to confirm that the produced glasses were made from robust glass-forming fluid. All these parameters will be discussed and evaluated in the current glassy system. In a further attempt, the ability of Se to form networks and the arrangement of bonds between the atoms that make up alloys have been used to explain changes in the values of these characteristics.

Experimental

The common melt quenching technique was used for the synthesis of bulk alloys of the chalcogenide glassy system $Se_{90}Pb_{10-x}Sn_x$ ($0 \leq x \leq 8$). This approach involved utilizing an electronic balance to weigh Se, Pb, and Sn elements with a 5N purity of 99.999% in the proper atomic mass percentage proportion. The chemicals were mixed and sealed in an evacuated (10^{-6} Torr) quartz ampoule to eliminate the probability of any reaction of alloy with oxygen at high temperatures. The assurance about the homogeneity of the resulting alloy is obtained by gradually heating the ampoule and its contents from room temperature (at a rate of 3–4 K min^{-1}) up to 1100 K and then maintaining this temperature for roughly 10 h while being frequently shaken. The molten samples were then speedily quenched in ice-cooled water to produce the wanted alloy in an amorphous state. The amorphous nature of the prepared samples was checked using SHIMADZU XRD-7000. In the past also, various workers have used XRD techniques and confirmed that lead-containing and chalcogen-rich alloys can be achieved in the glassy form [19–24].

After breaking the ampoules and carefully pulverizing the sample in a mortar and pestle to create a fine powder, the produced bulk glass was obtained. The thermal characterization of the prepared powder samples was done using DSC (NETZSCH DSC 200 *F3*). The five values of the heating rate β in the multiple of five (i.e., $\beta = 5\,n$; $n = 1, 2, 3, 4, 5$) in the range of ambient temperature to around 600 K were selected. This equipment has a temperature accuracy of 0.1 K. The DSC system was calibrated before measurements. The calibration was made using a high-purity standards material (i.e., indium) having a well-known melting point. The amount of the powdered samples used for thermal analysis was 5–8 mg. The nitrogen gas was used as a purging agent throughout the calorimetric measurements.

Results and discussion

Thermal stability

Non-isothermal DSC scans of the glassy system $Se_{90}Pb_{10-x}Sn_x$ ($0 \leq x \leq 8$) are shown in Fig. 1a at a heating rate of 15 K min^{-1}. Three regions are shown in Fig. 1a: the endothermic glass transition region, the exothermic crystallization region, and the endothermic melting region. Using these peaks, one can determine four characteristic temperatures (i.e., glass transition T_g, on-set T_c, and the peak T_p, crystallization temperatures, and melting
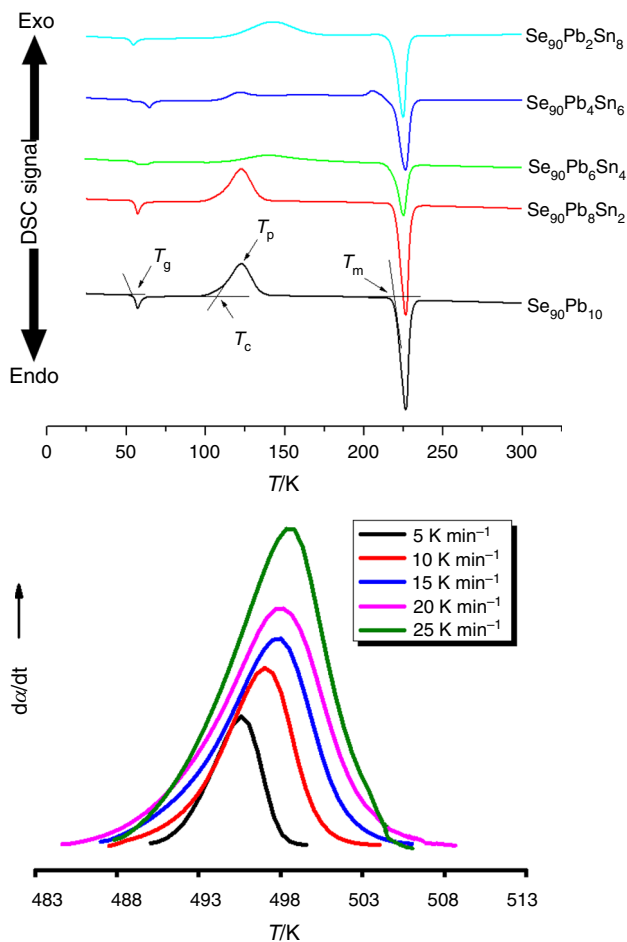
Fig. 1 **a** Non-isothermal DSC scans for $Se_{90} Pb_{10-x}Sn_x$ ($0 \leq x \leq 8$) glasses at a heating rate of 15 /Kmin^{-1}, and **b** Plots of (dα/dt) versus temperature at different heating rates for representative sample $Se_{90}Pb_6Sn_4$

temperature T_m). These DSC scans demonstrate that the glass/crystal phase transition occurs in all of the examined samples. The first endothermic peak accompanied by the second exothermic peak in each scan reveals the corresponding structural relaxation and devitrification of each alloy as a characteristic of the glass transition and crystallization phenomena. Further evidence that all of the examined glassy alloys are homogeneous comes from the single glass transition and single crystallization peaks that were detected [6]. For each heating rate, the values of the aforementioned characteristic temperatures are tabulated in Table 1. This table reveals the renowned shifting behavior of these characteristic temperatures toward the higher temperature side with increasing heating rate.

To check the validity of the data (i.e., the characteristics of kinetic temperatures), we have calculated the volume fraction α from the conversion curves of melting endotherms and obtained the value of (dα/dt) at different temperatures. Figure 1b shows such plots for a representative sample

Table 1 Values of the characteristic temperatures T_g, T_c, T_p, and T_{om} of $Se_{90} Pb_{10-x}Sn_x$ ($0 \leq x \leq 8$) at different values of heating rates β

Composition	β/Kmin^{-1}	T_g/K	T_c/K	T_p/K	T_{om}/K
$Se_{90}Pb_{10}$	5	323.8	371.4	382.6	493.1
	10	326.1	377.3	390.6	492.5
	15	327.5	380.6	395.6	492.7
	20	328.7	383.4	399.8	492.6
	25	329.4	385.6	404.1	492.5
$Se_{90}Pb_8Sn_2$	5	323.6	376.5	394.7	490.6
	10	326.0	379.0	404.8	490.4
	15	327.7	381.8	412.9	490.6
	20	328.8	384.1	419.0	489.8
	25	329.9	389.7	426.8	490.6
$Se_{90}Pb_6Sn_4$	5	322.2	373.5	395.2	491.7
	10	324.9	381.6	405.5	491.8
	15	326.3	385.2	412.1	490.9
	20	327.5	386.7	417.4	490.3
	25	328.4	389.3	423.3	490.5
$Se_{90}Pb_4Sn_6$	5	329.4	371.1	380.2	491.5
	10	331.9	377.7	387.8	491.2
	15	333.3	381.6	394.1	491.4
	20	334.7	384.5	398.4	490.8
	25	335.5	387.7	401.8	490.3
$Se_{90}Pb_2Sn_8$	5	319.3	377.4	397.6	491.9
	10	322.6	382.9	408.2	491.6
	15	324.1	387.0	415.4	490.4
	20	325.2	391.4	423.1	490.8
	25	326.2	393.1	428.9	490.4

$Se_{90}Pb_6Sn_4$ at different heating rates. We observe that the values of the peak melting temperatures (i.e., T_{mp}) obtained from both curves are in excellent agreement. The comparison of the results for the same representative sample is tabulated in Table 2 (Fig. 2).

The rigidity of the alloy structure is related to T_g and does not alone give any indication of the thermal stability [6]. As the stiffness of alloys is significantly extended and branched by a substantial number of limitations, they are oriented

Table 2 Comparison of the values of the peak melting temperatures of $Se_{90}Pb_6Sn_4$ alloy determined experimentally from calorimetric measurements and theoretically from conversion curves of the volume fraction of melting endotherms

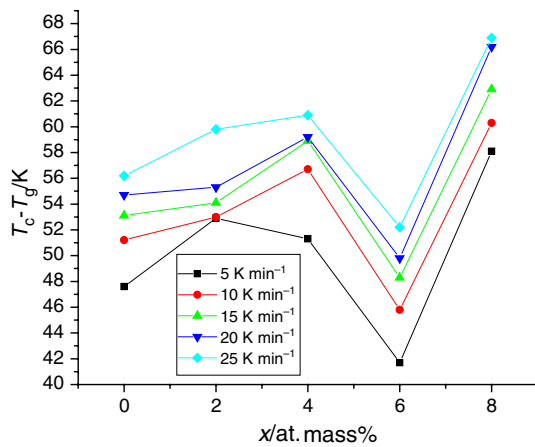| β/Kmin^{-1}	T_{pm}/K (Theoretical values)	T_{pm}/K (Experimental values)
5	495.5	495.7
10	497	497.2
15	497.5	497.7
20	498	498.1
25	498.3	498.5

Fig. 2 Dependence of Dietzel's temperature difference [i.e., $(T_c - T_g)$ parameter] on Sn content x

toward crystallization instead of converting into glassy structure when melt quenching occurs [11]. Dietzel [25] introduced the first glass criterion to estimate thermal stability by suggesting that the difference $(T_c - T_g)$ is a noble sign of thermal stability. This depends on the fact that whether the glass is stable (having T_c near to T_m) or unstable glass

(having T_c near to T_g). As a result, the nucleation process is delayed, thermal stability is increased, and glass formation is made easier as the difference between T_c and T_g increases [26]. Using this difference, two other criteria to evaluate thermal stability were obtained by Saad and Poulin [27]. The first is the weighted thermal stability H_g and the second is the S parameter, given by:

$$H_g = \frac{(T_c - T_g)}{T_g} \tag{1}$$

$$S = \frac{(T_c - T_g)(T_p - T_c)}{T_g} \tag{2}$$

The stability of the glass increases with the S-parameter value. This is because $(T_p - T_c)$ is connected to the devitrification rate of the glassy phases and S represents a barrier to their devitrification. Values of Dietzel temperature difference $(T_c - T_g)$, S-parameter, and H_g for the present glassy alloys have been calculated at all heating rates. These values are listed in Table 3. The non-monotonic compositional behavior of these parameters is shown in Figs. 3 and 4. It is clear from these figures that the thermal stability of the

Table 3 Values of $(T_c - T_g)$, H_g, S, K_p, T_{rg}, H_R, and F_i of $Se_{90}Pb_{10-x}Sn_x$ ($0 \le x \le 8$) at different values of heating rates β

Composition	β/Kmin^{-1}	$T_c - T_g$/K	H_g	S/K	K_p/min^{-1}	T_g/T_m	H_R	F_i
$Se_{90}Pb_{10}$	5	47.6	0.147	1.65	0.387	0.657	0.391	57.7
	10	51.2	0.157	2.09	0.743	0.662	0.444	40.0
	15	53.1	0.162	2.43	1.087	0.665	0.474	33.9
	20	54.7	0.166	2.73	1.419	0.667	0.501	30.5
	25	56.2	0.171	3.16	1.736	0.669	0.526	28.3
$Se_{90}Pb_8Sn_2$	5	52.9	0.163	2.98	0.260	0.660	0.463	51.9
	10	53.0	0.163	4.19	0.556	0.665	0.459	36.0
	15	54.1	0.165	5.13	0.713	0.668	0.497	30.5
	20	55.3	0.168	5.87	0.923	0.671	0.523	27.5
	25	59.8	0.181	6.73	1.113	0.672	0.593	25.5
$Se_{90}Pb_6Sn_4$	5	51.3	0.159	3.61	0.298	0.655	0.434	49.9
	10	56.7	0.175	4.17	0.567	0.661	0.515	34.6
	15	58.9	0.181	4.68	0.823	0.665	0.557	29.3
	20	59.2	0.181	5.55	1.070	0.668	0.570	26.4
	25	60.9	0.185	6.31	1.301	0.670	0.602	24.5
$Se_{90}Pb_4Sn_6$	5	41.7	0.127	1.15	0.375	0.670	0.346	54.1
	10	45.8	0.138	1.39	0.721	0.676	0.404	37.5
	15	48.3	0.145	1.81	1.047	0.678	0.440	31.8
	20	49.8	0.149	2.07	1.366	0.682	0.468	28.6
	25	52.2	0.156	2.19	1.678	0.684	0.509	26.6
$Se_{90}Pb_2Sn_8$	5	58.1	0.182	3.68	0.263	0.649	0.507	47.1
	10	60.3	0.187	4.73	0.500	0.656	0.555	32.6
	15	62.9	0.194	5.51	0.724	0.661	0.608	27.6
	20	66.2	0.204	6.45	0.930	0.663	0.666	24.9
	25	66.9	0.205	7.34	1.131	0.665	0.688	23.1
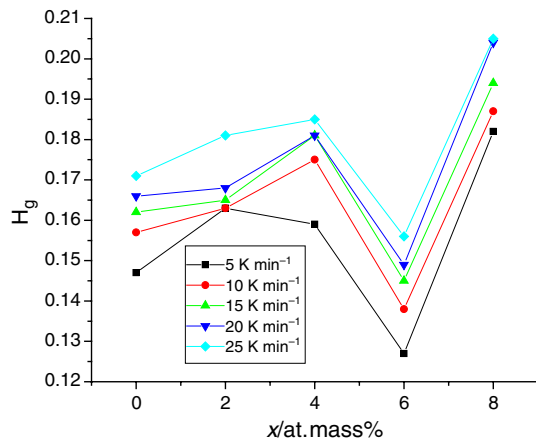
Fig. 3 Dependence of H_g parameter on Sn content x

Fig. 5 Plots of ln β vs. $1000/T_g$ for $Se_{90}Pb_{10-x}Sn_x$ ($0 \leq x \leq 8$) glasses
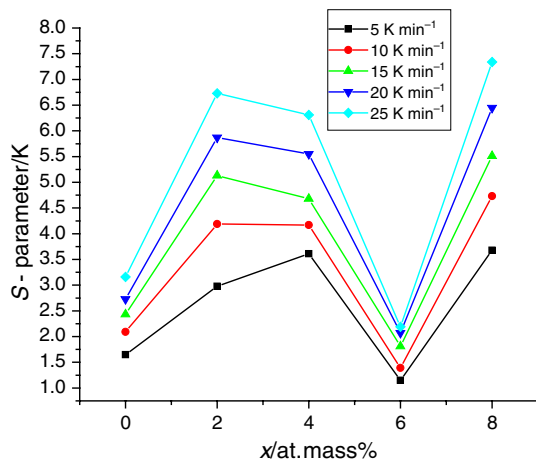
Fig. 4 Dependence of S parameter on Sn content x

Fig. 6 Plots of ln (β/T_g^2) vs. $1000/T_g$ for $Se_{90}Pb_{10-x}Sn_x$ ($0 \leq x \leq 8$) glasses

present ternary $Se_{90}Pb_{10-x}Sn_x$ glasses increases up to x = 4 at. mass% of Sn, then decreases at x = 6 at. mass% of Sn and a sharp rise occurred at x = 8 at. mass% of Sn. This is generally observed because of the non-uniform bonding arrangements between the atoms of different constituent elements of the samples in the composition range under study. Figures 3 and 4 reveal that the $Se_{90}Pb_2Sn_8$ sample is the best glass former and better thermally stable in the present case and so it offers high writability and archival storage for its possible application in phase-change optical memories. Further, it possesses a moderate melting point that makes this composition better for the cyclability of its stable layer stack.

The structural relaxation activation energy, linked to the glass transition, (E_t) is another crucial measure of thermal stability. Two familiar techniques proposed by Moynihan et al. [28] and Kissinger [29] are the most frequently used to calculate E_t from the variation of T_g with β. These procedures can be expressed by the following two equations:
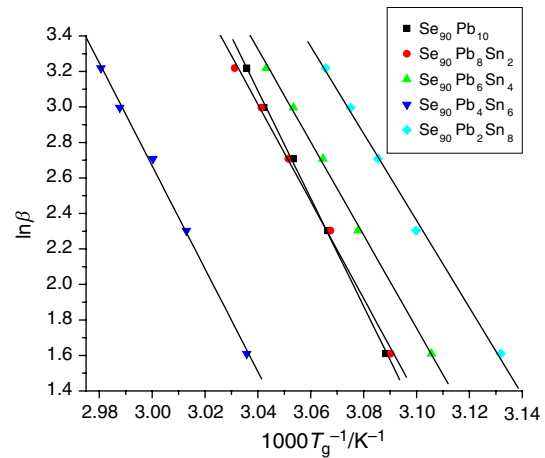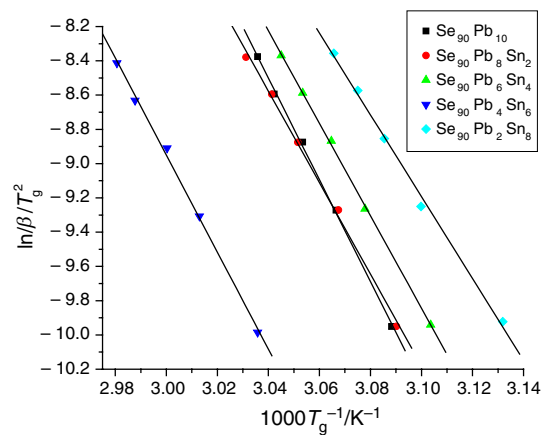
$$\frac{\partial(ln\beta)}{\partial(1/T_g)} = \frac{-E_t}{R} \tag{3a}$$

$$\frac{\partial\left(ln\beta/T_g^2\right)}{\partial(1/T_g)} = \frac{-E_t}{R} \tag{3b}$$

The value of E_t can be estimated by plotting ln β against $1/T_g$ for Eq. 3a and ln(β/T_g^2) against $1/T_g$ for Eq. 3b. These graphs are shown in Figs. 5 and 6 for all compositions. Table 4 lists the activation energy E_t values that were determined from the slopes of the generated straight lines. The energy required to cause an atom in one metastable state (or local minimum) in the glassy area to jump to another potential neighboring metastable state is referred to as E_t. During the structural relaxation process, E_t is engaged in molecular

Table 4 Values of glass transition activation energy E_t evaluated using two different methods and the parameters A and B of the Lasocka equation

Composition	Lasocka		Moynihan et al	Kissinger
	A_g/K	B_g/K	E_t/kJmol^{-1}	E_t/kJmol^{-1}
Se$_{90}$Pb$_{10}$	318.1±0.2	3.51±0.07	252.5±4.9	247.1±4.9
Se$_{90}$Pb$_8$Sn$_2$	317.2±0.3	3.89±0.13	227.5±6.8	222.1±6.8
Se$_{90}$Pb$_6$Sn$_4$	316.0±0.2	3.83±0.06	217.8±5.2	212.3±5.2
Se$_{90}$Pb$_4$Sn$_6$	323.2±0.3	3.80±0.12	241.2±6.7	235.6±6.7
Se$_{90}$Pb$_2$Sn$_8$	312.6±0.4	4.23±0.13	203.9±7.0	198.6±7.0

Fig. 7 Plots of T_g vs. ln β for Se$_{90}$Pb$_{10-x}$Sn$_x$ ($0 \le x \le 8$) glasses

mobility and atom readjustments at T_g. As a result, the most stable atoms are those that have a higher propensity to transition from one metastable state to another with lower internal energy and lower activation energy [30, 31]. The values of E_t that were discovered using the two approaches mentioned here are in strong agreement with one another. The observation of the lowest E_t value (corresponding to the maximum in thermal stability) the vice versa for the investigated glasses are in good agreement with the result above, which was reached using the values of ($T_c - T_g$), H_g, and S-parameter for the investigated glasses. Furthermore, Lasocka [32] introduced an empirical relation that expresses T_g in terms of β as follows:

$$T_g = A_g + B_g \log \beta \tag{4}$$

Lasocka's constants for this particular glass composition are A_g and B_g. While B_g is proportional to the length of time required by the system to reduce T_g, A_g indicates the glass transition temperature at a heating rate of 1 K min^{-1}. Further, the slope of the line drawn by Eq. (4) is denoted by B_g. Both A_g and B_g for each composition can be calculated from the plots of T_g versus ln β for all compositions under study. Figure 7 represents these plots and the evaluated values of A_g and B_g for all compositions are listed in Table 4. It is suggested that [33, 34], the value of B_g is related to the value of the relaxation activation energy E_t. The greater transitory receptivity of the localized configurational variations is observed when a glass has a high B_g value. This means that the glass network takes a smaller amount of energy to activate so it is more stable [33]. An analogous relationship between the Lasocka parameter B_g and the glass transition activation energy E_t has been observed in the present case. This shows that the glass Se$_{90}$Pb$_2$Sn$_8$ has a maximum value of B_g and a minimum value of E_t.

The temperature corresponding to the maximum crystallization rate is indicated by the crystallization rate factor K_p. It has been determined from the study of DSC curves using the following conditions [34]:
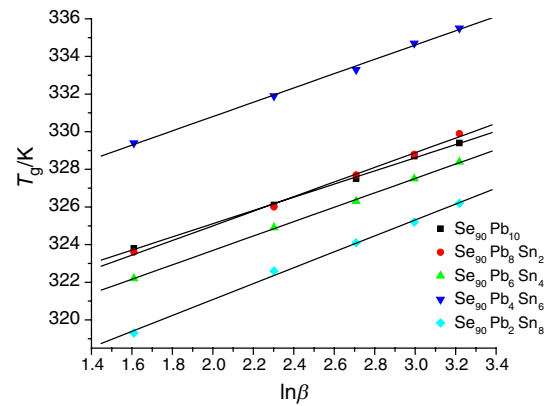
$$\frac{\beta E_c}{RT_p^2 K_p} = 1 \tag{5}$$

This relationship is viewed as an alternative method for determining the glass's stability. The symbols here have the same significance as they do throughout the text. The value of E_c in Eq. (5) is the mean of activation energies determined using the expressions of Kissinger, Takhor, and Augis–Bennett given as Eqs. 6a, 6b, and 6c respectively [29, 36, 37]:

$$\frac{\partial \left(\ln \beta / T_p^2 \right)}{\partial (1/T_p)} = \frac{-E_c}{R} \tag{6a}$$

$$\frac{\partial (\ln \beta)}{\partial (1/T_p)} = \frac{-E_c}{R} \tag{6b}$$

$$\frac{\partial \left(\ln \beta / T_p \right)}{\partial (1/T_p - T_0)} = \frac{-E_c}{R} \tag{6c}$$

In Eq. 6c, T_0 in the Augis–Bennett relation denotes the initial temperature (i.e., the ambient temperature at which the DSC experiment starts) of the sample (not the on-set temperature T_o).

Various authors [38–41] have suggested the modified form of the Augis–Bennett relation by ignoring the initial temperature as compared to the peak crystallization temperature:

$$\ln \left(\frac{\beta}{T_c} \right) = -\frac{E_c}{RT_c} + \ln K_o \tag{6d}$$

The benefit of the modification Augis–Bennett relation is that it makes the results independent of the laboratory temperature at which the calorimetric experiment is performed.
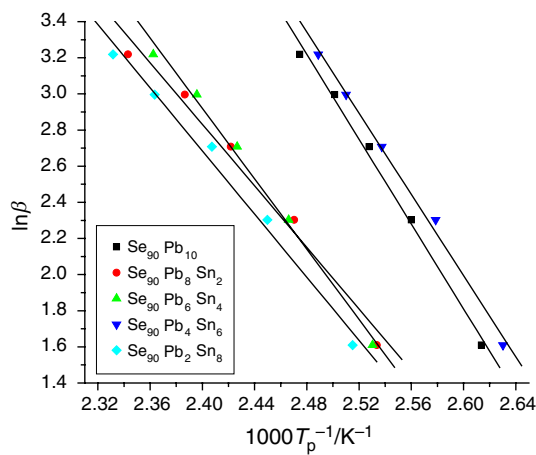
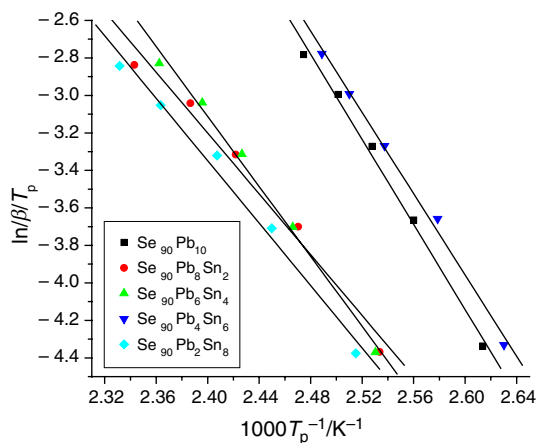**Fig. 8** Plots of lnβ vs. $1000/T_p$ for $Se_{90}Pb_{10-x}Sn_x$ $(0 \leq x \leq 8)$ glasses

Fig. 9 Plots of ln (β/T_p) vs. $1000/T_p$ for $Se_{90}Pb_{10-x}Sn_x$ $(0 \leq x \leq 8)$ glasses

Fig. 10 Plots of ln (β/T_p^2) vs. $1000/T_p$ for $Se_{90}Pb_{10-x}Sn_x$ $(0 \leq x \leq 8)$ glasses

Table 5 Values of crystallization activation energy E_c evaluated using three different methods for $Se_{90}Pb_{10-x}Sn_x$ $(0 \leq x \leq 8)$ glasses

Composition	$E_c/kJmol^{-1}$		
	Kissinger	Augis–Bennett	Takhor
$Se_{90}Pb_{10}$	91.0 ± 4.3	94.3 ± 4.3	97.6 ± 4.3
$Se_{90}Pb_8Sn_2$	64.0 ± 5.5	67.4 ± 5.4	70.8 ± 5.4
$Se_{90}Pb_6Sn_4$	74.1 ± 3.8	77.5 ± 3.8	80.9 ± 3.8
$Se_{90}Pb_4Sn_6$	86.9 ± 3.7	90.1 ± 3.7	93.4 ± 3.7
$Se_{90}Pb_2Sn_8$	65.8 ± 4.7	69.2 ± 4.7	72.7 ± 4.7

The crystallization activation energy E_c for each method, calculated from the slope of the plots shown in Figs. 8–10, are listed in Table 5. The activation energies of the glass transition/crystallization are found to be less after the incorporation of Sn and their compositional behavior for ternary alloys is non-uniform. It is widely accepted that the glass transition/crystallization activation energies are related to the movement of the molecular entities during structural relaxation near T_g and crystal growth near T_c respectively. The entrance of light element Sn (atomic mass 118.7 g mol⁻¹) in the glass network of parent glass by replacing comparatively heavy element Pb (atomic mass 207.2 g mol⁻¹) facilitates the easy movement of structural units by reducing the mean atomic masses of ternary alloys, thereby, reducing the values of E_t and E_c.

By averaging the estimated values of K_p at the various heating rates (see Table 3), the average values (i.e., $(<K_p>)$ of K_p are obtained, which are then presented in Fig. 11a
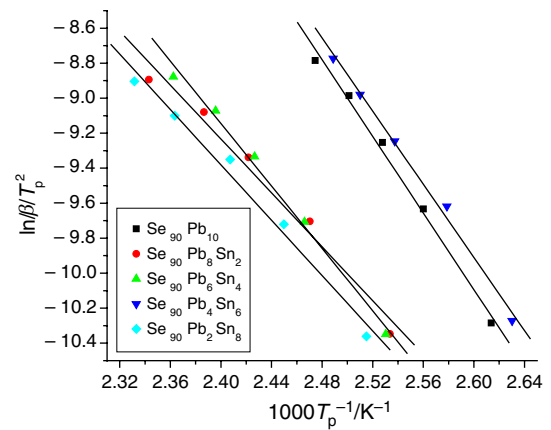
for all compositions. The glass with the greatest stability will reportedly crystallize at the slowest rate [42]. A close estimation indicates that the mean values $<K_p>$ of K_p has a decreasing sequence which is almost opposite to that of the mean value of the stability parameter S. This reveals that a phase-change material goes through amorphous to crystalline phase change at a lower crystallization rate if it has a higher thermal stability.

Glass-forming ability

This parameter is a measurement of how simple it is to create glass. The lowered glass transition temperature T_{rg}, which is supplied as the first parameter used to estimate the GFA, can be expressed as [43, 44]:

$$T_{rg} = \frac{T_g}{T_m} \tag{7}$$

According to Turnbull's [45] theory, the glass-forming capacity should decline with a lower T_{rg} for a given composition. Table 3 lists the computed T_{rg} values for the current samples at various values of β. This table shows that all of these values are near 0.66 and fall within the acceptable
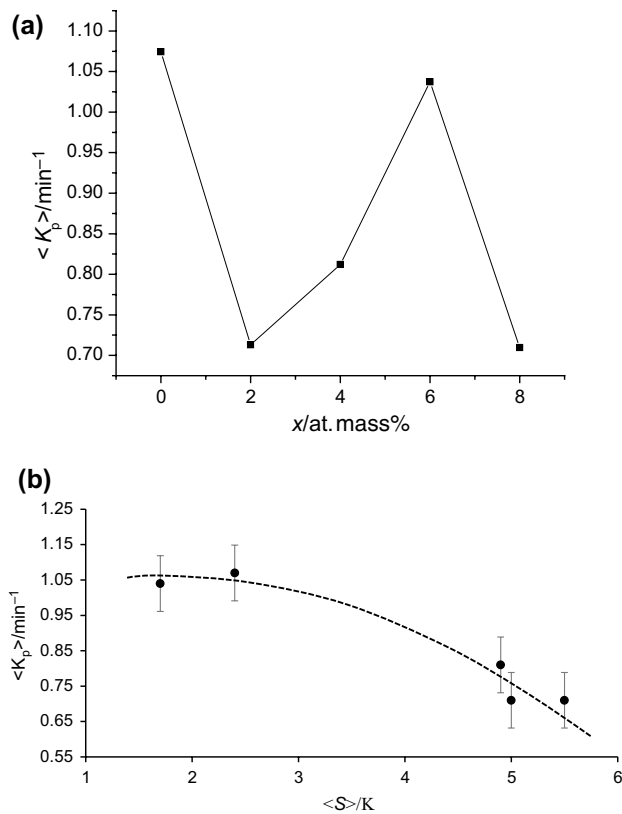
(a)

(b)

Fig. 11 Variation of the average value of crystallization rate factor $<K_p>$ with **a** Sn content x, and **b** average value of thermal stability parameter $<S>$ (curved line is guided to eyes)

range. Additionally, to the ongoing effort, many additional investigations [6, 11, 12, 46, 47] demonstrated that T_{rg} possesses almost always the same value (mostly = 2/3) in most of the glasses. Consequently, it fails to take into account variations in GFA among various glass compositions. It is, therefore, crucial to find another GFA indication to distinguish between the various glasses' compositions. For this, the criterion proposed by Hruby [48] is as follows:

$$H_R = \frac{T_c - T_g}{T_m - T_c} \qquad (8)$$

This is known as Hruby's parameter which provides the chance of acquiring a glass by rapid cooling of the melt. Table 3 tabulates the H_R values at different values of β. Earlier studies indicate that glasses having $H_R \geq 0.4$ developed readily with small rates of quenching [48]. However, it is a difficult task to obtain glasses having $H_R \leq 0.1$ so higher rates of quenching are expected. According to Table 3, at the identical heating rate, the maximum H_R value arises at 8 at% of Sn, and all H_R values are higher than 0.4. This indicates that $Se_{90}Pb_{10-x}Sn_x$ alloys $(0 \leq x \leq 8)$ are effective glass formers and that Se–Pb–Sn glasses in the studied range are simple to create

when Sn is added at the expense of Pb. Interestingly, H_R is also the maximum for the $Se_{90}Pb_{10-x}Sn_x$ sample.

Fragility index

The concept of fragility was introduced by Angell, during the process of cooling of super-cooled liquid. It is explained as the rate at which a supercooled liquid's viscosity increases at T_g [49–51]. As the temperature gradually drops, the viscosity increases exponentially, preventing the atoms and molecules from settling into long-range periodic arrangements, and leading to the formation of glass [51]. Since strong glasses have resistance to structural deterioration and typically have a lower enthalpy of structural relaxation kinetics, fragile glasses are substances with non-directional interatomic or intermolecular connections [52]. The viscosity of strong glass-forming liquids follows an Arrhenius temperature dependency with virtually uniform perceived activation energy for viscous flow. The viscosity for liquids that may break glass, however, exhibits a temperature relationship that is distinctly non-Arrhenius. The perceived activation energy for viscous flow also shows abrupt fluctuations, going from an extremely small value beyond the melting point to an extremely elevated one when nearing the glass transition [14]. By observing how quickly the relaxation time shrinks as the temperature increases around T_g, one can determine how fragile a glass-like material is. Further, we can compute the fragility by using the following relation [53]:

$$F_i = \frac{E_t}{RT_{g.}\ln\beta} \qquad (9)$$

We have used the average values of E_t determined by Eqs. 3a and 3b in Fragility calculations. According to theory, F_i ranges from 16 for robust systems to 200 for fragile ones. Chalcogenide glassy systems lie in the middle region between these two limits. Covalent directed linkages that form a spatial network define the strong glass-forming liquids. Fragile liquids, on the other hand, are made up of molecular units having Van der Waals bonding to hold them with each other isotopically [20]. For all samples and heating rates, the fragility index was determined and is shown in Table 32. This table reveals that glassy $Se_{90}Pb_{10-x}Sn_x$ $(0 \leq x \leq 8)$ alloys attain the lowest limit (≈ 16) of F_i values, which suggests that all of the glassy alloys in the system under study were produced by strong glass-forming liquids.

Conclusions

The impact of tin incorporation on the kinetic parameters of glass transition/crystallization of binary $Se_{90}Pb_{10}$ glass as a parent sample has been examined. The entry of tin in the parent glass network at the expense of lead Pb makes it

easier for structural units to move around because it lowers the mean atomic masses of ternary alloys, which lowers the values of E_t and E_c. Different kinetic parameters (e.g., H_g, S, K_p, T_{rg}, H_R, etc.) of the parent sample are changed noticeably, however, the changes are found to be non-monotonous. It is noticed that E_t initially decreases with Sn content but it exhibits a maximum value of 6 atomic mass percentage of Sn after which it again decreases. This result agrees fairly well with that obtained from thermal stability parameters and indicates that $Se_{90}Pb_4Sn_6$ glass has the lowest stability in the composition range of the study. In the existing ternary $Se_{90}Pb_{10-x}Sn_x$ glasses, the thermal stability value shows a maximum value for $x = 8$ at. mass% of Sn in a non-linear compositional dependence. The crystallization rate ($<K_p>$) mean values are lowest at $x = 2$ and 8, indicating that these two compositions require a lengthy time to fully crystallize. Their resistance to devitrification is therefore at its peak, while the composition with 6 at. mass% of Sn exhibits the highest rate of crystallization and the lowest resistance to devitrification.

The computed values of the fragility index show that all of the samples in the current study are produced by strong glass-forming liquids. The maximum value of $<K_p>$ and E_c occurs for $Se_{90}Pb_4Sn_6$ glass which crystallizes earlier than the other compositions. Investigation of the glass-forming ability GFA criteria and fragility index indicates that the studied glasses are simple to create and have been produced by strong glass-forming liquids.

Authors contribution Mousa M.A. Imran, Omar A. Lafi contributed to plotting graphs and writing—original draft. Amal Rabah, A. Al-Bqoor contributed to calorimetric measurements. A. Dahshan, H. I. Elsaeedy contributed to formal analysis and writing—final draft. N. Mehta contributed to conceptualization, materials synthesis, and writing—revised version of the draft.

References

1. Jiang Z-H, Zhang Q-Y. The structure of glass: a phase equilibrium diagram approach. Prog Mater Sci. 2014;61:144–215.
2. Sharma V, Sharda S, Sharma N, Katyal SC, Sharma P. Chemical ordering and electronic properties of lone pair chalcogenide semiconductors. Prog Sol Stat Chem. 2019;54:3–44.
3. Lafi OA, Imran MMA, Abu-Shaweesh NI, Al-Kurdi FM, Khatatbeh IK. Effect of chemical ordering on the crystallization behavior of $Se_{90}Te_{10-x}Sn_x$ (x= 2, 4, 6, and 8) chalcogenide glasses. J Phys Chem Solids. 2014;75:790–5.
4. Kasap SO, Rowlands J, Fogal B, Kabir MZ, Belev G, Sidhu N, Polischuk B, Johanson RE. Progress in the science and technology of direct conversion a-Se X-ray sensors. J Non-Cryst Sol. 2002;299–302:988–92.
5. Singh AK. A short overview on advantage of chalcogenide glassy alloys. J Non-Oxide Glasses. 2012;3:1–4.
6. Mehta N, Tiwari RS, Kumar A. Glass forming ability and thermal stability of some Se-Sb glassy alloys. Mater Res Bull. 2006;41:1664–72.
7. Weinberg MC. Glass-forming ability and glass stability in simple systems. J Non-Cryst Sol. 1994;167:81–8.
8. Lafi OA, Imran MMA, Abdullah MK. Glass transition activation energy, glass-forming ability and thermal stability of $Se_{90}In_{10-x}Sn_x$ (x = 2, 4, 6 and 8) chalcogenide glasses. Physica B. 2007;395:69–75.
9. Abd-Elnaiem AM, Abbady G. A thermal analysis study of melt-quenched Zn_5Se_{95} chalcogenide glass. J Alloys Comp. 2020;818: 152880.
10. Shaaban ER, Yahia IS, Fadel M. Effect of composition on the thermal stability for Ge–In–Se intermediate compound. J Alloys Comp. 2009;469:427–32.
11. Kumar A, Fouad SS, El-Bana MS, Mehta N. Thermal analysis of cadmium addition on the glass transition and crystallization kinetics of Se-Te-Sn glassy network. J Therm Anal Calorim. 2018;131:2491–501.
12. Angell CA. Relaxation in liquids, polymers and plastic crystals–strong/fragile patterns and problems. J Non-Cryst Sol. 1991;131–133:13–31.
13. Senapati U, Varshneya AK. Viscosity of chalcogenide glass-forming liquids: an anomaly in the 'strong' and 'fragile' classification. J Non-Cryst Sol. 1996;197:210–8.
14. Fan GJ, Choo H, Liaw PK. Fragility of metallic glass-forming liquids: a simple thermodynamic connection. J Non-Cryst Sol. 2005;351:3879–2883.
15. Chen S-W, Huang T-Y, Hsu Y-H, Kroupa A. Phase diagram of the Pb-Se-Sn system. J Electron Mater. 2020;49:4714–29.
16. Hawarat EO, Imran MMA, Lafi OA, Juwhari HK, Lahlouh BI, Chandel N, Mehta N. Effect of Sn content on some optical properties of $Se_{90}Pb_{10-x}$ thin films. Opt Mater 2020;100:109672.
17. Zobac O, Zemanova A, Chen S-W, Kroupa A. CALPHAD-type assessment of the Pb-Se-Sn system. J Phase Equilib Diffus. 2022;43:243–55.
18. Sushama D, George A. Structural studies of $Se_{100-X}Pb_X$ (X = 01, 5 & 10) glasses. AIP Conf Proc 2011;1391:775–777.
19. Wakkad MM, Raheem MMA, Mohamed HA, Hamed NI, The crystallization kinetic studies of the $Sn_5Ge_{10}Se_{85-x}Pb_x$ (2.5≤x≤20 at. %) chalcogenide glasses. Sohag J Sci. 2023;8:163–174.
20. Hairan R, Azizi AT. Synthesis and X-ray diffraction study of $Se_{79}Te_{20}Pb_1$ chalcogen glass. J Res Appl Sci Biotech. 2023;2:89–92.
21. Saraswat VK, Tanwar N, Saxena NS. Modifications in band gap & dc conductivity of ternary chalcogenide glasses by addition of lead. J Non-Oxide Glass. 2012;4:55–61.
22. Kumar P, Modgil V, Rangra VS. The far-infrared study of Ge modified Sn–Se–Pb chalcogenide glasses. J Non-Oxide Glass. 2012;6:27–35.
23. Khan ZH, Khan SA, Alvic AM. A study of glass transition and crystallization behavior in $Ga_{15}Se_{85-x}Pb_x$ (0 ≤ x ≤ 6) chalcogenide glasses. Acta Phys Pol. 2013;123:80–6.
24. Deepika, Jain PK, Rathore KS, Saxena NS. Structural characterization and phase transformation kinetics of $Se_{58}Ge_{42}xPb_x$ (x = 9, 12) chalcogenide glasses. J Non-Cryst Sol. 2009;355:1274–80.
25. Dietzel A. Glass structure and glass properties. Glasstech Berl. 1968;22:41–50.
26. Lafi OA, Imran MMA. Compositional dependence of thermal stability, glass-forming ability and fragility index in some Se–Te–Sn glasses. J Alloys Comp. 2011;509:5090–4.
27. Saad M, Poulin M. Glass forming ability criterion. Mater Sci For. 1987;19–20:11–8.

28. Moynihan CT, Easteal AJ, Wilder J, Tucker J. Dependence of the glass transition temperature on heating and cooling rate. J Phys Chem. 1974;78:2673–7.

29. Kissinger HE. Reaction kinetics in differential thermal analysis. Anal Chem. 1957;29:1702–6.

30. Imran MMA, Saxena NS, Bhandari D, Husain M. Glass Transition Phenomena, Crystallization Kinetics and Enthalpy Released in Binary $Se_{100-x}In_x$ (x = 2, 4 and 10) Semiconducting Glasses. Phys Stat Sol A. 2000;181:357–68.

31. Imran MMA, Bhandari D, Saxena NS. Kinetic studies of bulk $Ge_{22}Se_{78-x}Bi_x$ (x = 0, 4 and 8) semiconducting glasses. J Therm Anal Calor. 2001;65:257–74.

32. Lasocka M. The effect of scanning rate on glass transition temperature of splat-cooled $Te_{85}Ge_{15}$. Mater Sci Eng. 1976;23:173–7.

33. Saraswat V, Pal SK, Mehta N, Kumar A, Imran MMA. Thermal analysis of novel third-generation phase-change materials with zinc as a chemical modifier. RSC Adv. 2023;13:3602.

34. Kumar H, Mehta N, Singh K. Calorimetric studies of glass transition phenomenon in glassy $Se_{80-x}Te_{20}Sn_x$ alloys. Phys Scr. 2009;80:065602.

35. Gao YQ, Wang W. On the activation energy of crystallization in metallic glasses. J Non-Cryst Sol. 1986;81:129–34.

36. Takhor RL. Determining the suitability of nucleating agents for glass-ceramics. In Advanced in Nucleation and Crystallization in Glasses, Hench LL, Frieman SW (ed.), American Ceramic Society, Westerville (1971), p 166.

37. Augis J, Bennett J. Calculation of the Avrami parameters for heterogeneous solid-state reactions using a medication of the Kissinger method. J Therm Anal Calorim. 1978;13:283–92.

38. Patial BS, Thakur N, Tripathi SK. On the crystallization kinetics of In additive Se–Te chalcogenide glasses. Thermochim Acta. 2011;513:1–8.

39. Imran MMA. Crystallization kinetics, glass transition kinetics, and thermal stability of $Se_{70-x}Ga_{30}In_x$ (x = 5, 10, 15, and 20) semiconducting glasses. Phys B. 2011;406:482–7.

40. Abdel-Wahab F. Observation of phase separation in some Se–Te–Sn chalcogenide glasses. Phys B. 2011;406:1053–9.

41. Srivastava S, Zulfequar M, Agrahari SK, Kumar A. Kinetics of crystallization in glassy $Se_{70}Te_{30-x}Zn_x$ using DSC technique. Phys B. 2008;403:3429–33.

42. Abdel-Rahim MA, Hafiz MM, Shamekh AM. A study of crystallization kinetics of some Ge–Se–In glasses. Physica B. 2005;369:143–54.

43. Kauzmann W. The nature of the glassy state and the behavior of liquids at low temperatures. Chem Rev. 1948;43:219–56.

44. Clavaguera-Mora MT. Glassy materials: thermodynamic and kinetic quantities. J Alloys Comp. 1995;220:197–205.

45. Turnbull D. Under what conditions can a glass be formed? Contemporary Phys. 1969;10:473–88.

46. Rao V, Chandel N, Mehta N, Dwivedi DK. Effect of antimony on glass transition and thermal stability of $Se_{78-x}Te_{18}Sn_2Sb_x$ (x = 0, 2, 4 & 6 at %) multi component glassy alloys. J Therm Anal Calorim. 2018;134:915–22.

47. Abdel-Rahim MA, Gaber A, Abu-Sehly AA, Abdelazim NM. Crystallization study of Sn additive Se–Te chalcogenide alloys. Thermochim Acta. 2013;566:274–80.

48. Hurby A. Evaluation of glass forming tendency by means of DTA. Czech J Phys B. 1972;22:1187–93.

49. Lafi OA, Imran MMA, Abdullah MK. Chemical bond approach to glass transition temperature and crystallization activation energy in $Se_{90}In_{10-x}Sn_x$ ($2 \leq x \leq 8$) semiconducting glasses. Mater Chem Phys. 2008;108:109–14.

50. Angell CA. The old problems of glass and the glass transition, and the many new twists. Proc Natl Acad Sci USA. 1995;92:6675–82.

51. Angell CA, Ngai KL, McKenna GB, McMillan PF, Martin SW. Relaxation in glass-forming liquids and amorphous solids. J Appl Phys. 2000;88:3113–57.

52. Abd-el Salam MN, Shaaban ER, Benabdallah F, Hussein AMA, Mohamed M. Experimental and theoretical studies of glass and crystallization kinetics of semiconducting $As_{40}Se_{40}Ag_{20}$ chalcogenide glass. Phys B. 2021;608: 412745.

53. Xia Y, Yuan B, Gulbiten O, Aitken B, Sen S. Kinetic and calorimetric fragility of chalcogenide glass-forming liquids: Role of shear vs enthalpy relaxation. J Phys Chem B. 2021;125:2754–60.